Available online at www.sciencedirect.com
SCIENCE DIRECT®
Physics Letters A 340 (2005) 275–280
PHYSICS LETTERS A
www.elsevier.com/locate/pla

Spontaneous symmetry breaking in photonic lattices: Theory and experiment

P.G. Kevrekidis [a,*], Zhigang Chen [b,c], B.A. Malomed [d], D.J. Frantzeskakis [e], M.I. Weinstein [f,g]

[a] *Department of Mathematics and Statistics, University of Massachusetts, Amherst, MA 01003-4515, USA*
[b] *Department of Physics and Astronomy, San Francisco State University, CA 94132, USA*
[c] *TEDA College, Nankai University, Tianjin 300457, China*
[d] *Department of Interdisciplinary Studies, Faculty of Engineering, Tel Aviv University, 69978 Tel Aviv, Israel*
[e] *Department of Physics, University of Athens, Panepistimiopolis, Zografos, 15784 Athens, Greece*
[f] *Department of Applied Physics and Applied Mathematics, Columbia University, New York, NY 10025, USA*
[g] *Mathematical Sciences Research, Bell Laboratories, Murray Hill, NJ 07974, USA*

Received 5 March 2005; accepted 11 March 2005

Available online 29 March 2005

Communicated by V.M. Agranovich

Abstract

We examine an example of spontaneous symmetry breaking in a double-well waveguide with a symmetric potential. The ground state of the system beyond a critical power becomes asymmetric. The effect is illustrated numerically, and quantitatively analyzed via a Galerkin truncation that clearly shows the bifurcation from a symmetric to an asymmetric steady state. This phenomenon is also demonstrated experimentally when a probe beam is launched appropriately into an optically induced photonic lattice in a photorefractive material.

1. Introduction

Spontaneous symmetry breaking (SSB) is a ubiquitous phenomenon in modern physics. Manifestations of the SSB have been found in diverse areas, ranging from liquid crystals [1] to quantum dots [2], and from coupled semiconductor lasers [3] to the pattern dynamics of *Dictyostelium discoideum* [4]. Of particular interest is the recent experimental demonstration of spatial symmetry-breaking instability in the interaction of laser beams in optical Kerr media [5]. For an overview of the time-honored history of the SSB in field theory, see the reviews [6].

There has recently been a huge amount of activity and many advances in the study of light dynamics in photonic structures, such as materially fabricated pho-

* Corresponding author.
E-mail address: kevrekid@math.umass.edu (P.G. Kevrekidis).

0375-9601/$ – see front matter
doi:10.1016/j.physleta.2005.03.038

tonic crystals (PCs) and optically induced photonic lattices in nonlinear media; see, for example, [7,8]. This is motivated by the enormous potential for applications ranging from highly tunable telecommunications elements to cavity QED experiments. Among many phenomena explored are nonlinear effects associated with propagation, localization, and discretization of light in optically-induced photonic lattices [9], including the formation of lattice solitons in one [10,11] and two dimensions [12–14], and discrete vortex solitons [15,16].

In this Letter, our aim is to study a prototypical example of SSB for a setting of the nonlinear Schrödinger (NLS) type with an effective symmetric double-well potential, i.e., a prototypical "dual-core" photonic lattice. As the optical power is increased, we identify a symmetry-breaking bifurcation in the system's ground state, with a transfer of stability to asymmetric states, with more power concentrated in one core than in the other. This, generally, resembles theoretically predicted SSB bifurcations in diverse dual-core optical systems of more traditional types, such as dual-core fibers (see Ref. [17]), linearly coupled $\chi^{(2)}$ waveguides and dual-core fiber gratings [18]. We present an analysis using a Galerkin truncation based on the eigenfunction basis of the underlying linear double-well problem, which accurately predicts the bifurcation in the present context. Then, we demonstrate such SSB experimentally in an optically-induced waveguide lattice in photorefractive media. Our method of prediction and analysis of SSB is quite general. For example, NLS equations of the Gross–Pitaevskii and nonlinear-Hartree types play a fundamental role in the study of Bose–Einstein condensation [19]. In the latter context, a rigorous variational proof showing that a SSB transition must occur is given in [20], and a complete study of the SSB transition in a special one-dimensional (1D) model was developed in Ref. [21].

The Letter is structured as follows. In Section 2, we introduce the NLS model and its connection to the optical lattice problem. The stability of stationary states and the SSB bifurcation are studied numerically. In Section 3, the finite-mode (Galerkin) approximation and the prediction of SSB following from it are elaborated. Section 4 details the observation of the SSB in the experiment. Section 5 contains a summary of our findings and conclusions.

2. Model and numerical results

Our model is based on (1D) equations that describe the propagation of light in a photorefractive crystal [22]; see also the recent exposition in [23]. The 1D version makes it possible to demonstrate the SSB in its simplest/most fundamental form. Specifically, we consider a probe beam that is extraordinarily polarized, while a strong ordinarily polarized beam creates an effective lattice potential for the probe. Then, the equation for the spatial evolution of a slowly varying amplitude U of the probe beam is

$$iU_z + \frac{1}{2k_0 n_e} U_{xx} - \frac{1}{2} k_0 n_e^2 r_{33} \frac{E_0}{1 + I_0(x) + |U|^2} U = 0. \tag{1}$$

In Eq. (1), z and x are the propagation distance and transverse coordinate, respectively, k_0 is the wavenumber of the probe beam in the vacuum, n_e is the refractive index along the extraordinary axis, r_{33} is the electro-optic coefficient for the extraordinary polarization, E_0 is the bias electric field, and $I_0(x)$ is the intensity of the ordinarily polarized beam, subject to modulation in the transverse direction (all intensities are normalized with respect to the crystal's dark irradiance, I_d). Measuring z in units of $2k_0 n_e$ and E_0 in units of $1/(k_0^2 n_e^4 r_{33})$, Eq. (1) can be cast in a dimensionless form,

$$iU_z + U_{xx} - \frac{E_0}{1 + I_0(x) + |U|^2} U = 0. \tag{2}$$

Nonlinear bound states of Eq. (2) are localized solutions of the form $U(x,z) = u(x)\exp(i\mu z)$, where u obeys

$$u_{xx} - \frac{E_0}{1 + I_0(x) + |u|^2} u = \mu u. \tag{3}$$

We consider the case of an effective symmetric two-hump potential

$$I_0(x) = V_0 \left[\exp\left(-\frac{(x-a)^2}{2\epsilon^2} \right) + \exp\left(-\frac{(x+a)^2}{2\epsilon^2} \right) \right], \tag{4}$$

corresponding to a superposition of two Gaussian beams. Solutions to Eq. (3) with $I_0(x)$ given by (4) were found via the Newton's method on a finite-difference grid. The linear stability of the stationary states is determined by the eigenvalues and eigenvectors, $\{\lambda, (a,b)\}$ of the linearized equation, obtained

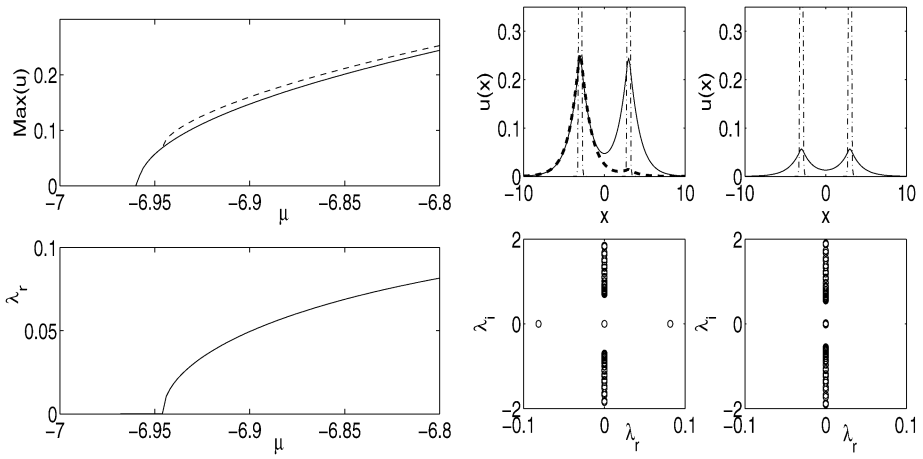

Fig. 1. The symmetry-breaking bifurcation which gives rise to asymmetric solutions in Eq. (3) with the potential of Eq. (4). The parameters are $\epsilon = 0.1$, $V_0 = (\pi\epsilon)^{-1/2} \approx 1.784$, $a = 3$, and $E_0 = 7.5$. The solid and dashed lines in the top subplot of the left panel show the amplitudes of the symmetric and asymmetric (bifurcating) solutions vs. μ. The bottom subplot displays the unstable real eigenvalue for the symmetric-solution branch existing past the bifurcation point, at $\mu > -6.94575$. The right panel shows, in its top subplots, examples of the symmetric and asymmetric solutions (solid and thick dashed lines, respectively) for $\mu = -6.8$ (left) and $\mu = -6.95$ (right), respectively. In the latter case (i.e., before the bifurcation point), only the symmetric branch (solid line) exists. The background profile of $I_0(x)$ is indicated by a dash-dotted line. The bottom subplots show the respective results of the linear stability analysis around the symmetric solution in the complex plane (λ_r, λ_i) of the stability eigenvalues. An eigenvalue with a positive real part (in the left panel) implies instability of the solution.

by the substitution of $U(x,z) = \exp(i\mu z)\{u(x) + \delta[\exp(-\lambda z)a(x) + \exp(-\lambda^\star z)b^\star(x)]\}$ into (1) and linearization in the small parameter δ. For very weak nonlinearity, the profile of the ground state follows the symmetry of the double-well potential (4). We searched for a symmetry-breaking bifurcation as the optical power of the nonlinear bound state, $N = \int_{-\infty}^{+\infty} |u(x)|^2\,dx$ was increased.

The results are summarized in Fig. 1 (for $E_0 = 7.5$, cf. Ref. [23]). The top left panel of the figure shows the amplitude of the solution as a function of μ. The solid and dashed lines correspond, respectively, to the symmetric and asymmetric solutions, the latter bifurcating from the former (SSB) at a critical power N_c. The bottom left panel displays the real part λ_r of the most unstable eigenvalue of the symmetric solution, which shows that the symmetry-breaking bifurcation destabilizes the symmetric solution. This occurs through the appearance of a pair of real eigenvalues for $N > N_c \equiv 0.15167$, or, equivalently, for $\mu > \mu_c \equiv -6.94575$, when the solution's amplitude (maximum value of $|u(x)|$) exceeds 0.06924. The asymmetric solution emerging at the bifurcation point is stable. The right panel of Fig. 1 shows details of the relevant solutions and their stability for $\mu > \mu_c$ (left) and $\mu < \mu_c$ (right). In fact, two asymmetric solutions arise, being mirror images of each other, i.e., the bifurcation is super-critical.

The evolution of the stable and unstable stationary solutions was investigated in direct simulations of Eq. (2). Fig. 2 displays the results for the unstable symmetric solution with $\mu = -6.5$ and stable symmetric one with $\mu = -6.95$. As initial conditions, we took highly accurate numerically obtained stationary states perturbed by a uniformly distributed random perturbation of an amplitude 0.0001. In the unstable case, the manifestation of the SSB is very clear; as a result of the growth of the unstable eigenmode triggered by the small perturbation, the nearly symmetric state with $\mu = -6.5$ evolves into a stable asymmetric one; see the dashed line in Fig. 2. On the other hand, the stable symmetric ground state for $\mu = -6.95$ remains unchanged (solid line in Fig. 2).

3. Analytical results

To analytically examine SSB in Eq. (2), we develop a Galerkin-type method generally applicable to

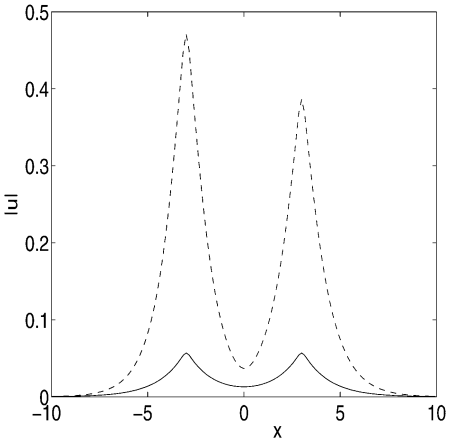

Fig. 2. The profile of the field modulus $|u|$ for the same propagation distance but different symmetric initial conditions: a stable one (solid line) for $\mu = -6.95$, resulting in the stable symmetric state, and an unstable one for $\mu = -6.5$, resulting in the asymmetric state shown by the dashed line. The potential is the same as for Fig. 1.

related models. It is convenient to define $U(x,z) \equiv u(x,z)\exp(i\mu z)$, replacing Eq. (2) with

$$iu_z = \mu u - u_{xx} + \frac{E_0}{1 + I_0(x) + |u|^2}u. \tag{5}$$

Numerics corroborate our expectation that, for sufficiently large separation a between the potential wells, the bifurcation occurs at low powers, i.e., when Eq. (5) is close to its linear counterpart. It is therefore natural to seek a representation of $u(x,z)$ in terms of the basis of the eigenfunctions of the double-well potential: $\omega_j v^{(j)} = -v^{(j)}_{xx} + \frac{E_0}{1+I_0(x)}v^{(j)}$. Numerical solution of this equation reveals two localized eigenstates of the double-well potential with corresponding eigenvalues $\omega_0 = 6.95886$ and $\omega_1 = 6.98631$. The former eigenmode is even and the latter one is odd.

We expect that the bifurcation shown in Fig. 1 may occur, in the nonlinear equation (5), at μ close to $-\omega_0$, and the emerging asymmetric solution may be close to a superposition of the two above-mentioned localized linear eigenmodes. We explore this possibility by means of a Galerkin truncation based on these modes:

$$u(x,z) = c_0(z)v^{(0)}(x) + c_1(z)v^{(1)}(x), \tag{6}$$

where c_0 and c_1 are assumed small. Substitution of (6) into (5), projecting onto the linear eigenmodes and retaining leading-order nonlinear terms yields the following finite-dimensional reduction:

$$i\dot{c}_0 = (\mu + \omega_0)c_0 - a_{00}|c_0|^2 c_0 - a_{01}\big(2|c_1|^2 c_0 + c_0^{\star}c_1^2\big), \tag{7}$$

$$i\dot{c}_1 = (\mu + \omega_1)c_1 - a_{11}|c_1|^2 c_1 - a_{01}\big(2|c_0|^2 c_1 + c_1^{\star}c_0^2\big), \tag{8}$$

where the overdot stands for d/dz, $a_{kl} \equiv E_0 \times \int_{-\infty}^{+\infty}[v^{(k)}(x)]^2[v^{(l)}(x)]^2[1 + I_0(x)]^{-2}\,dx$, and $a_{00} \approx 0.86302$, $a_{01} \approx 0.89647$, $a_{11} \approx 0.93958$.

Substituting further $c_j \equiv \rho_j \exp(i\phi_j)$, and taking into regard the conservation of the total norm, $\rho_0^2 + \rho_1^2 = N$, we reduce Eqs. (7) and (8) to a system of two real ordinary differential equations:

$$\dot{\rho}_0 = a_{01}\rho_0^2\rho_1 \sin(2\Delta\phi), \tag{9}$$

$$\Delta\dot{\phi} = -\Delta\omega + a_{11}\rho_1^2 - a_{00}\rho_0^2 + a_{01}\big(2 + \cos(2\Delta\phi)\big)\big(\rho_0^2 - \rho_1^2\big), \tag{10}$$

where $\Delta\phi \equiv \phi_1 - \phi_0$ and $\Delta\omega \equiv \omega_1 - \omega_0$. Since we are interested in real solutions of the underlying equation (5), we will confine our considerations to steady states with $\Delta\phi = 0 \pmod{\pi}$. Then, from Eq. (10) one can easily find that no solution bifurcates from $\rho_0 = 0$; however, solutions with $\rho_1 \neq 0$ can bifurcate from the symmetric ones with $\rho_0^2 = N$ and $\rho_1 = 0$. These are the solutions that we are interested in, as they may account for the SSB, due to the inclusion of the odd eigenfunction $v^{(1)}(x)$ in Eq. (6). The critical value of the norm at which the bifurcation occurs, is found from Eqs. (9) and (10) to be

$$N_c = (3a_{01} - a_{00})^{-1}|\Delta\omega|. \tag{11}$$

This simple prediction is the main finding of the analysis. One can also find, from Eqs. (7) and (8), the critical propagation constant μ_c at which the SSB is expected,

$$\mu_c = -\omega_0 + a_{00}(3a_{01} - a_{00})^{-1}|\Delta\omega|. \tag{12}$$

Eqs. (11) and (12) finally predict the occurrence of the bifurcation at $N_c = 0.01503$ and $\mu_c = -6.94589$, in remarkable agreement with the numerical simulations reported above. In particular, the relative error in N_c is considerably less than 1% in the worst case, and the error in the prediction of μ_c is $\approx 0.002\%$.

4. Experimental results

Experiments were performed in a biased photorefractive crystal (SBN:60, $5 \times 5 \times 20$ mm^3) illuminated by a partially coherent beam periodically modulated with an amplitude mask. This spatially modulated beam is ordinarily polarized, so it experiences only a weak nonlinearity and induces a stable square waveguide lattice in the biased crystal [13,24]. The principal axes of the lattice are oriented in horizontal and vertical directions. A Gaussian beam, split off from the same laser source, is used as a coherent probe beam. Contrary to the experiments with discrete solitons [12–14], the probe beam is focused inter-site, i.e., between two lattice sites in the vertical direction (to avoid any anisotropic effects such as those from self-bending, since the crystalline c-axis is oriented in the horizontal direction). The probe beam is extraordinarily polarized, propagating collinearly with the lattice through the crystal. The polarization configuration is chosen so that the probe would experience strong nonlinearity but the induced lattice remains nearly undisturbed during propagation [22]. To demonstrate the SSB, all experimental conditions were kept unchanged, except that the intensity of the probe beam was increased gradually. Typical experimental results are presented in Fig. 3. They were obtained with a lattice of 45 μm nearest neighbor spacing. When the intensity of the probe beam is low, its energy tunnels into two waveguides symmetrically, as seen in the transverse patterns of the probe beam in Fig. 3(a)–(c). Above a threshold value of the input intensity, the intensity pattern of the probe beam at output becomes asymmetric, as shown in Fig. 3(d). The bifurcation from a symmetric to an asymmetric output is also clearly visible in the vertical profiles of the probe beam displayed in Fig. 3. These results are related to the even-mode solitons [11], or the two parallel in-phase solitons [25], observed previously in optically-induced lattices, which were found to be unstable. Here we demonstrated a clear bifurcation from symmetric to asymmetric states due to the SSB, which is more relevant to the symmetry-breaking instability of a two-humped, self-guided laser beam, observed in a different nonlinear-optical system [5]. It should be clarified that since in the present setting a periodic lattice is present, the system is, strictly speaking, not a double-well potential. This implies that for very long propagation distances, power will tunnel to other wells of the potential and is likely to result to antisymmetric configurations similar to the ones observed in [26]. However, for the relatively short propagation distances (and the initial conditions) examined here, the lattice is *effectively* a double-well system.

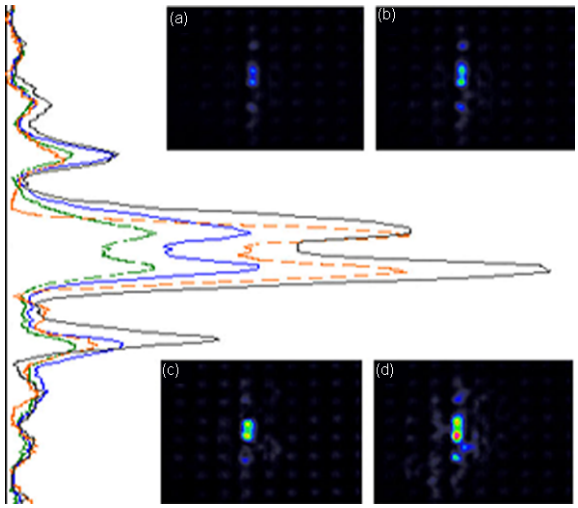

Fig. 3. Experimental demonstration of SSB in an optically induced photonic lattice. From (a) to (d), shown are the transverse intensity patterns of the probe beam (initially a fundamental Gaussian beam) at an intensity (normalized to the lattice intensity) of 0.1, 0.2, 0.3 and 0.5. The bias field was kept at 2 kV/cm, and all other parameters were fixed. The left side shows the corresponding vertical beam profiles.

5. Conclusion and discussion

We have studied numerically and analytically the bifurcation from a symmetric to an asymmetric ground state in an equation of the NLS type. The equation models the propagation of a probe beam through an optically-induced periodic lattice in a photorefractive nonlinear crystal. A double-well potential locally approximates the spatial shape of the lattice guiding the probe beam. The ground-state profile breaks its symmetry at a critical power, N_c. The transition is accompanied by destabilization of the symmetric state. The threshold, N_c, as well as other essential features of the SSB bifurcation, are very well approximated by the finite mode (Galerkin) approximation based on a superposition of the symmetric and antisymmetric lin-

ear states of the double-well potential. In parallel to the theoretical analysis, we have reported the experimental observation of these phenomena in optically-induced photonic lattices in a photorefractive crystal.

The analysis detailed herein can be adapted to models of Gross–Pitaevskii or nonlinear-Hartree types, which are central to modeling symmetry breaking and other phenomena in BECs [20,21,27]. See also Ref. [28], for such an analysis when a BEC is loaded into a combination of a magnetic trap and an optical lattice.

Finally, although the simple two-mode truncation was used here in the one-dimensional geometry, generalizations to arbitrary dimensions and incorporation of higher-order modes can be developed to describe more complex bifurcations, in both static and time-dependent settings, as well as coupling to radiation waves [29]. These are directions currently under investigation.

Acknowledgements

This work was partially supported by NSF-DMS-0204585, NSF-CAREER, and the Eppley Foundation for Research (P.G.K.). AFOSR, ARO and NSFC (Z.C.), the Israel Science Foundation through the grant No. 8006/03 (B.A.M.), and NSF-DMS-0412305 (M.I.W.). We are indebted to Todd Kapitula for valuable discussions.

References

[1] A.G. Vanakaras, D.J. Photinos, E.T. Samulski, Phys. Rev. E 57 (1998) R4875.
[2] C. Yannouleas, U. Landman, Phys. Rev. Lett. 82 (1999) 5325.
[3] T. Heil, et al., Phys. Rev. Lett. 86 (2001) 795.
[4] S. Sawai, Y. Maeda, Y. Sawada, Phys. Rev. Lett. 85 (2000) 2212.
[5] C. Cambournac, et al., Phys. Rev. Lett. 89 (2002) 083901.
[6] R. Brout, hep-th/0203096;
F. Englert, hep-th/0203097.
[7] J.D. Joannopoulos, R.D. Meade, J.N. Winn, Photonic Crystals: Modeling the Flow of Light, Princeton Univ. Press, Princeton, 1995.
[8] Yu.S. Kivshar, G.P. Agrawal, Optical Solitons: From Fibers to Photonic Crystals, Academic Press, San Diego, 2003.
[9] D.N. Christodoulides, F. Lederer, Y. Silberberg, Nature 424 (2003) 817.
[10] J.W. Fleischer, et al., Phys. Rev. Lett. 90 (2003) 023902.
[11] D. Neshev, et al., Opt. Lett. 28 (2003) 710.
[12] J.W. Fleischer, et al., Nature (London) 422 (2003) 147.
[13] H. Martin, et al., Phys. Rev. Lett. 92 (2004) 123902.
[14] Z. Chen, et al., Phys. Rev. Lett. 92 (2004) 143902.
[15] D.N. Neshev, et al., Phys. Rev. Lett. 92 (2004) 123903.
[16] J.W. Fleischer, et al., Phys. Rev. Lett. 92 (2004) 123904.
[17] C. Paré, M. Florjańczyk, Phys. Rev. A 41 (1990) 6287;
B.A. Malomed, et al., Phys. Rev. E 53 (1996) 4084.
[18] W.C.K. Mak, B.A. Malomed, P.L. Chu, Phys. Rev. E 55 (1997) 6134;
W.C.K. Mak, B.A. Malomed, P.L. Chu, J. Opt. Soc. Am. B 15 (1998) 1685.
[19] F. Dalfovo, et al., Rev. Mod. Phys. 71 (1999) 463;
L.P. Pitaevskii, S. Stringari, Bose–Einstein Condensation, Oxford Univ. Press, Oxford, 2003.
[20] W.H. Aschenbacher, et al., J. Math. Phys. 43 (2002) 3879.
[21] R.K. Jackson, M.I. Weinstein, J. Stat. Phys. 116 (2004) 881.
[22] N.K. Efremidis, et al., Phys. Rev. E 66 (2002) 046602.
[23] J. Yang, New J. Phys. 6 (2004) 47.
[24] Z. Chen, K. McCarthy, Opt. Lett. 27 (2002) 2019.
[25] J. Yang, et al., Opt. Lett. 29 (2004) 1662.
[26] R. Morandotti, et al., Phys. Rev. Lett. 83 (1999) 2726;
U. Peschel, et al., J. Opt. Soc. Am. B 19 (2002) 2637.
[27] K.W. Mahmud, J.N. Kutz, W.P. Reinhardt, Phys. Rev. A 66 (2002) 063607.
[28] T. Kapitula, P.G. Kevrekidis, Bose–Einstein Condensates in the presence of a magnetic trap and optical lattice, available at http://www.math.unm.edu/~kapitula/papers/publications.html.
[29] A. Soffer, M.I. Weinstein, nlin.PS/0308020, Rev. Math. Phys., in press.